Chinese Chemical Letters 31 (2020) 1511–1515

Contents lists available at ScienceDirect

Chinese Chemical Letters

journal homepage: www.elsevier.com/locate/cclet

Communication

Efficient antimicrobial properties of layered double hydroxide assembled with transition metals *via* a facile preparation method

Mengxue Li[a,*], Li Li[b], Sijie Lin[a]

[a] College of Environmental Science and Engineering, Shanghai Institute of Pollution Control and Ecological Security, Key Laboratory of Yangtze River Water Environment, Tongji University, Shanghai 200092, China
[b] Australian Institute of Bioengineering and Nanotechnology, The University of Queensland, Brisbane, QLD 4072, Australia

ARTICLE INFO

Article history:
Received 28 June 2019
Received in revised form 16 September 2019
Accepted 24 September 2019
Available online 27 September 2019

Keywords:
Layered double hydroxides
Transition metals
Facile synthesis
Antibacterial activity
Synergistic mechanism

ABSTRACT

Mg^{2+} in MgAl-layered double hydroxides nanoparticles was substituted with different divalent transition metal ions (MAl-LDHs, M: Mg^{2+}, Cu^{2+}, Ni^{2+}, Co^{2+}, and Mn^{2+}) *via* a facile method to be used as antibacterial agents. The phase structural and morphological characterizations of MAl-LDHs were investigated by XRD, FTIR spectroscopy and TEM. The results have shown that all of MAl-LDHs had typical layered structures except MnAl-LDH which contained Mn_3O_4 phases. Particular morphology of MnAl-LDH with ellipsoids, spherical and rod-like structure and CuAl-LDH with rod-like shape existed. IC_{50} (the concentrations providing 50% antibacterial activity) values of CuAl-LDH, NiAl-LDH, CoAl-LDH, and MnAl-LDH in broth dilution tests were ~800-1500 μg/mL. Dosages of CuAl-LDH, CoAl-LDH, and MnAl-LDH with >10 mm inhibition zone in disk diffusion tests were ~150–300 μg/disk. Antibacterial mechanism of MAl-LDHs may be attributed to the synergistic factors including effected surroundings, surface interactions, morphology of particles, ROS and metal ions. The results indicate a facile method to synthesis LDHs based effective antibacterial agents with the potential application in the area of water treatment and antibacterial coating.

Overuse of antibiotics leads to emergence of drug-resistant bacteria. Thus, the development of a new class of inorganic antibacterial agents is necessary [1]. Recently, several kinds of inorganic materials assembled with the transition metal ions as antibacterial agents, including zinc, copper, nickel, cobalt and manganese, attract more and more attentions [2–4]. It is well known that the action of these antibacterial materials is dependent on the coordination with transition metal ions. Meanwhile, positive charged nanocarriers with high specific surface area are speculated to improve adhesion toward the negative charged surface of bacteria and thus increase their antimicrobial activity [5]. Therefore, positive charged nanoparticles assembled with transition metal ions might play a vital role during the antibacterial application.

Layered double hydroxides (LDHs) are one of low-cost bactericide compared with Au, Ag, TiO_2 *etc*. LDHs composed of brucite-like $Mg(OH)_2$ sheets are known as inorganic synthetic clays. The general chemical formula of positively charged LDHs is $[M_{1-x}^{II}M_x^{III}(OH)_2]^{x+}(A^{n-})_{x/n}\cdot zH_2O$ (M^{II}, M^{III} and A^{n-} : bivalent metal ions, trivalent metal ions and anions). The flexibility in composition and uniform distribution of metal cations make LDHs especially attractive for preparation of nanocomposite materials [6]. Besides, LDHs have a number of advantageous characteristics such as good biocompatibility, low cytotoxicity, high chemical stability, controllable particle sizes, varied functionality, high loading capacities, wide availability and the protection of biomolecules in the interlayers. The studies of LDHs are in the fields of adsorption, catalysis and biotechnology *etc*. [7]. Recently, very few researches have been conducted on the antimicrobial activity of pure LDHs as MgAl-LDH, MgFe-LDH and ZnAl-LDH [8–10]. However, in these researches, high dosages (316-14,000 μg/mL) and tedious preparation procedures (heating >80 °C or >2 h aging time) of LDHs hamper their antibacterial application.

To avoid these defects, the Mg^{2+} in the brucite type layers of Mg-LDHs could be substituted with the different antibacterial transition metal ions *via* a facile method. Cu, Ni, Co and Mn ions have been widely used for the preparation of inorganic antimicrobial agents due to their efficient antimicrobial activity [11–14]. The toxicity of Al ions to bacteria was the lowest among all the high valent cations tested [15]. Thus, Mg, Mn, Cu, Ni and Co assembled in Al-based LDHs (MAl-LDHs, M: Mg, Mn, Cu, Ni and Co) with facile

* Corresponding author.
E-mail address: limengxue@tongji.edu.cn (M. Li).

https://doi.org/10.1016/j.cclet.2019.09.047

synthesis and excellent performance against both Gram-negative (*Escherichia coli)* and Gram-positive bacterium (*Staphylococcus aureus),* is urgently needed to contribute practical antimicrobial use.

Accordingly, the objectives of this work were to: (1) Synthesize MAl-LDHs nanoparticles by a facile method (Scheme 1A(a)); (2) determine antibacterial activity *via* broth dilution tests and disk diffusion tests (Scheme 1A(b)); (3) reveal antibacterial mechanism towards bacterial cells (Scheme 1B). This research has demonstrated that efficient antibacterial behavior of Al-based LDHs assembled with Cu, Ni, Co, and Mn was obtained. Moreover, this work is carried out to improve understanding of LDH based antimicrobial agents with the different chemical composition.

MAl-LDH nanoparticles containing various transitional metals were prepared *via* a facile method. XRD results in Fig. 1a indicated that MgAl-LDH, CuAl-LDH, NiAl-LDH and CoAl-LDH exhibited typical (003) and (006) peaks of LDH, suggesting the formation of layered LDHs [16]. The values of a and c were calculated in the range of 2.93–3.06 Å and 24.1–26.5 Å in agreement with the literature report (Table S1 in Supporting information) [17]. The thickness of MAl-LDHs in c-axis was 1.9–6.0 nm, which can be evaluated by the Scherrer equation referring to the (003) Bragg reflection (Table S1). Based on thickness in c-axis, the number of layers of MAl-LDHs was recorded as 2.1-6.8. The slightly different lattice parameters of MgAl-LDH, CuAl-LDH, NiAl-LDH and CoAl-LDH may be due to the different atomic radius of the metals (Mg^{2+}, Cu^{2+}, Ni^{2+} and Co^{2+}) (Table S1) [18]. Moreover, compared with previous reports, the reduction in thickness and layers may be attributed to quick treatment without aging process which could influence the layer stacking [19–22].

Interestingly, MnAl-LDH displayed different phase structure as shown in Fig. 1a. MnAl-LDH had LDH phases (20.3°) and Mn_3O_4 phases (16.9°, 29.3°, 31.1°, 33.0°, 36.3°, 39.0°, 44.6°, 52.0°, 58.8°, 60.6°, 64.8°) [23]. The mixed phases were ascribed to oxidation of MnAl-LDH under air in the presence of NaOH, according to the below equation [24].

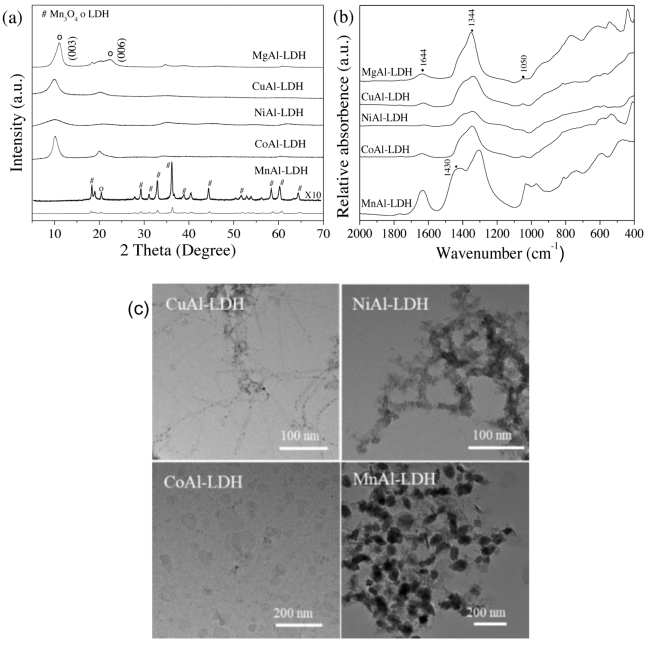

Fig. 1. (a) XRD patterns of MAl-LDHs. (b) The FTIR spectra of MAl-LDHs. (c) The TEM images of CoAl-LDH, CuAl-LDH, NiAl-LDH and MnAl-LDH.

$$6Mn^{2+} + 12OH^- + O_2 = 2Mn_3O_4 + 6H_2O$$

However, the relatively weaker intensity of the peaks of MnAl-LDH than that of MgAl-LDH, CuAl-LDH, NiAl-LDH and CoAl-LDH manifested a low crystallinity.

As listed in Table S1, all MAl-LDH nanoparticles were positive charged with the zeta potentials in the range of 32.1–40.1 mV [25], which may be helpful for LDHs electrostatic attraction negatively

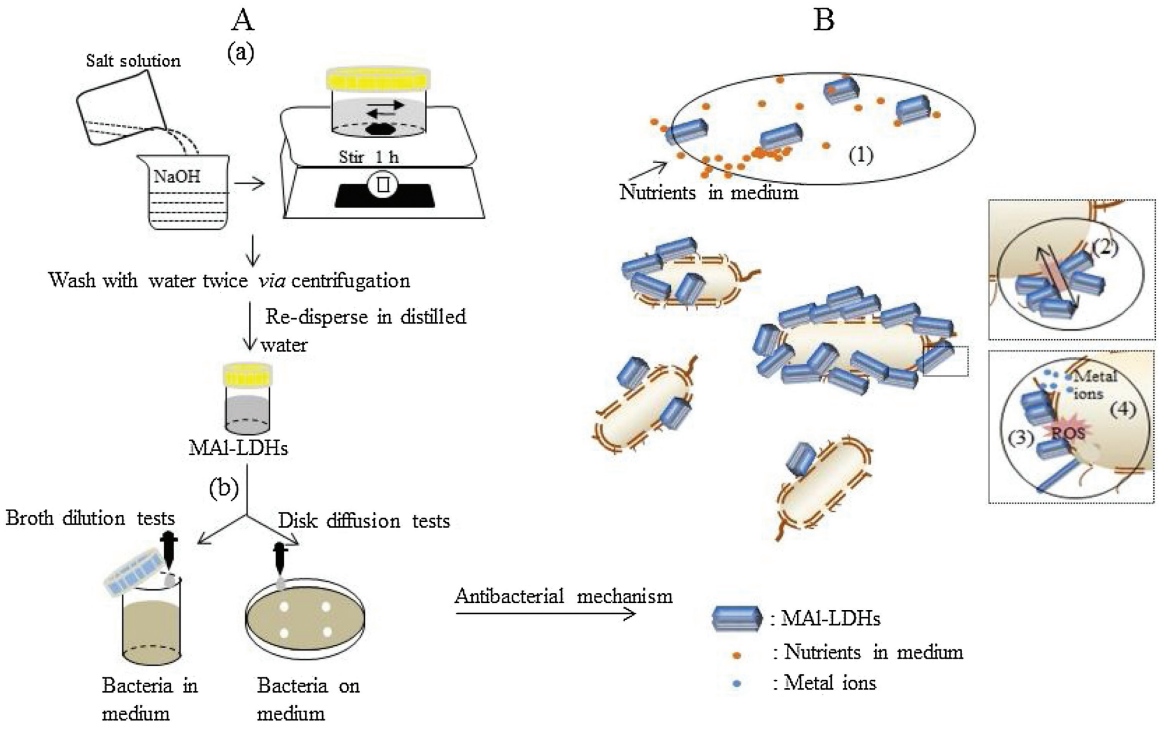

Scheme 1. Preparation strategy and antibacterial experiments of MAl-LDHs (A), A schematic illustration of possible antibacterial mechanism of MAl-LDHs against *E. coli* (B).

charged bacteria. Zeta potential is an important parameter for the colloidal stability of nanoparticles in suspension. Zeta potential of ~30 mV is required as a minimum for physically stable nanoparticle suspensions [26]. Thus, MAl-LDH nanoparticles prepared in this work were colloidally stable.

The FTIR absorption spectrums of MAl-LDHs were displayed in Fig. 1b. The bands characteristic to M–OH and M–O bond stretching for MAl-LDHs were below 1000 cm^{-1}. The broad features of interlayer water molecules were observed near 1640 cm^{-1} [27]. The bands of NO_3^- groups in the interlayer space presented at 1344 and 1050 cm^{-1} corresponding to the ν_3 and ν_1 stretching vibration, receptivity [28]. The absorption peak of MnAl-LDH at 1344 cm^{-1} was split into one more peak at 1430 cm^{-1} ($\nu_{as}(NO_2)$), which might be due to the decomposition of the NO_3^- groups with the formation of Mn_3O_4 [29]. The result was consistent with the formation of Mn_3O_4 phases in XRD.

The morphology of MAl-LDH was observed under TEM (Fig. 1c and Fig. S1a in Supporting information). MgAl-LDH and CoAl-LDH possessed uniform hexagonal platelets with the mean size around 50 nm (Fig. 1c and Fig. S1a). CuAl-LDH displayed rod-like shape with uncertain length (Fig. 1c) [30]. These nanorods tended to aggregate for typical LDH materials. And many dots were found on the nanorods, which may be Cu nanoparticles [31]. The morphology of NiAl-LDH showed of crystallites like crumpled films (Fig. 1c) [20]. The irregular morphology of NiAl-LDH samples may be attributed to short aging time during preparation process. MnAl-LDH samples in Fig. 1c had ellipsoids, spherical and a few rod-like particles with ~100 nm in size, similar to the morphology of Mn_3O_4 in accord with XRD patterns and FTIR spectra in Figs. 1a and b [32]. The particles were also found attached to each other to form agglomeration.

The broth dilution test has laid basics for antibacterial application in water. The biocidal efficacy of MAl-LDHs was evaluated by the broth dilution method for Gram-negative (*E. coli)* and Gram-positive (*S. aureus)* bacteria (Fig. 2). The antibacterial activity of all MAl-LDH samples exhibited in a dose-dependent manner, as shown in Fig. 2. The antimicrobial efficacy of MAl-LDHs increased with increasing concentration of MAl-LDHs. As shown in Fig. 2a, when the concentration of MAl-LDHs is below 800 μg/mL, MAl-LDHs had no obvious antibacterial activity. When the concentration of MAl-LDHs increased up to 1500 μg/mL, CuAl-LDH and MnAl-LDH showed the best bacterial inhibition towards *E. coli* compared to MgAl-LDH, NiAl-LDH and CoAl-LDH. However, NiAl-LDH and CoAl-LDH exhibited the limited antibacterial activity towards *E. coli* at 1500 μg/mL, while MgAl-LDH had no antibacterial ability. As shown in Fig. 2b, MnAl-LDH and CoAl-LDH showed 73% inhibition towards *S. aureus* at 1500 μg/mL. NiAl-LDH and CuAl-LDH exhibited the moderately active against *S. aureus* at 1500 μg/mL. But MgAl-LDH did not affect *S. aureus* growth even at the concentration of 1500 μg/mL.

The disk diffusion tests were done to be benefit for antibacterial application in the area of antibacterial coating. The corresponding size of inhibition zone of MAl-LDHs was showed in Table S2 (Supporting information). The highest antimicrobial activity towards *E. coli* and *S. aureus* was observed with CuAl-LDH at 150–300 μg/disk. Comparatively, CoAl-LDH, NiAl-LDH and MnAl-LDH produced smaller diameter of inhibition zone against bacteria, while MgAl-LDH produced no inhibition zone.

Based on above tests, IC_{50} (the concentrations providing 50% antibacterial activity) values of MAl-LDH samples towards bacteria were summarized in Table S3 (Supporting information). CoAl-LDH, MnAl-LDH, CuAl-LDH and NiAl-LDH showed the obvious antibacterial activities towards bacterial growth at ~800-1500 μg/mL. Moreover, CoAl-LDH, MnAl-LDH and CuAl-LDH in the concentration range of 150–300 μg/disk showed inhibition zone large than 10 mm towards bacteria (Table S3). The results of disk diffusion tests were a bit different with those of broth dilution tests, which could be attributed to diffusivity of MAl-LDHs. The agglomerated MAl-LDHs could have an effect on their diffusivity into agar [33]. The weaker bactericidal activity of MnAl-LDH in disk tests than that in broth tests may be attributed to the difficult diffusivity of agglomerated particles into agar (Fig. 1c).

Antibacterial tests demonstrate that MAl-LDHs had high efficiency as bactericides at low amounts by the broth dilution and disk diffusion tests, compared with similar solids such as LDHs or clays (Table 1) [8-10, 34-38]. Based on antibacterial mechanism of similar solids such as LDHs or clays (Table 1) and other antibacterial agents [39], the antibacterial activity of MAl-LDHs may depend on the combination of several factors such as effected surroundings, surface interactions, morphology, ROS and metal ions.

As proposed previously [40], nanoparticles with size smaller than 50 nm could be internalized by bacteria. However, TEM images in Fig. 1c displayed that MAl-LDHs with size larger than 100 nm attached on bacteria wall with large aggregates without internalization of MAl-LDHs. Thus, the contribution of MAl-LDHs uptake into bacteria to the antibacterial activity seems impossible.

MAl-LDHs at high concentrations may reduce nutrients in the medium by adsorbing on surfaces of particles to alter the physicochemical properties of a specific environment, which would indirectly affect the bacterial growth (Scheme 1B(1)) [41]. Meanwhile, electrostatic interactions between cationic MAl-LDHs and negatively charged bacterial surface could cause bacterial growth inhibition. MgAl-Cl-LDHs nanoparticles bound to the cell wall of bacteria were found (Fig. S1c in Supporting information). Similarly, MAl-LDHs precipitation staying firmly on the bacterial surfaces may have a directly effect on the biological activities of bacteria leading to block the transport channels for nutrient and waste recycling (Scheme 1B(2)) [42]. Furthermore, excessive deposition of particles on the surface may result in membranes

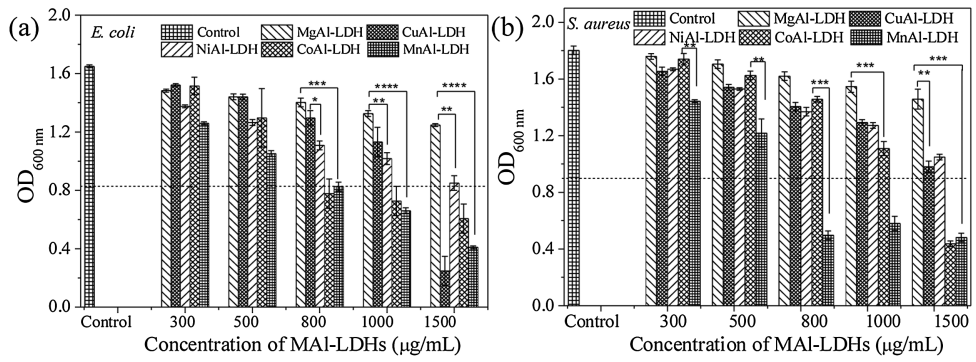

Fig. 2. Antibacterial activity towards (a) *E. coli* and (b) *S. aureus* in the presence of MAl-LDHs.

Table 1
Comparison of antibacterial activity of samples in literatures.

Samples	IC_{50} values (μg/mL)	Dosages with >10 mm inhibition zone (μg/disk)	Major antibacterial mechanism	References
MAl-LDHs	~800–1500	~150–300	Effected surroundings; Surface interactions; Morphology; ROS; Metal ions	This study
MgAl-LDH	2500	–	Surface interactions	[10]
MgAl-LDH	2511	–	Surface interactions	[8]
MgFe-LDH	316			
ZnAl-LDH	8000-14000	–	Surface interactions; Metal ions	[9]
Natural clay	80000	–	Metal ions; ROS; pH	[34]
Modified clay	>140000	–	Surface interactions; Metal ions	[35]
Iron-clay	>500000	–	Surface interactions; ROS; Metal ions	[36]
Montmorillonite-based particles	25000	–	Surface interactions; Metal ions	[37]
Ag-montmorillonite	–	>1000–2500	Surface interactions; Metal ions	[38]

disturbance and disorder. Thus, at the low concentration (< 800 μg/mL), low toxicity of MAl-LDH nanoparticles may be ascribed to limited attached particles on the surface of bacteria (Table 1). When concentration of LDHs increased up to 1500 μg/mL, huge amounts of LDHs may be completely adhered to bacteria and fully covered the bacteria wall with thick layers, resulting in efficient inhibition of bacteria growth.

As for MnAl-LDH, antibacterial activity could be attributed to additional reactive oxygen species (ROS) produced by Mn_3O_4, such as $O_2^{\bullet -}$, H_2O_2 and $^{\bullet}OH$ [43] (Scheme 1B(3)). Additionally, it is possible that the morphology of nanomaterials could affect the antibacterial activity. Rod-like nanoparticles easily penetrated into cell walls of bacteria, thus, enhancing the antibacterial efficiency [44]. In this case, the morphology of the CuAl-LDH and MnAl-LDH may contribute to the bactericidal efficacy (Scheme 1B(3)). But aggregation of CuAl-LDH and MnAl-LDH may restrict rod-like nanoparticles to independent entry.

Another possible antimicrobial mechanism may be the release of metal ions, which may diffuse into the bacterial cells to affect amino acid metabolism and enzyme system [45,46]. The antimicrobial activity of metal ions was determined (Fig. S2 in Supporting information). No antibacterial activity towards *E. coli* and *S. aureus* was observed in the presence of Cu^{2+}, Ni^{2+} and Mn^{2+} at 40–80 μg/mL, while obvious antibacterial efficacy of Co^{2+} was obtained. However, ICP results indicated no bivalent ions (Co^{2+}) released from the CoAl-LDH powder. Based on previous reports [8], a small amount of metal ions (<10 μg/mL) could be dissolved from LDHs. And according to the results in our group [47], LDHs also dissolved limited metal ions (2–4 μg/mL). Thus, limited metal ions dissolved from MAl-LDHs showed slightly toxicity to bacteria (Scheme 1B(4)).

Thus, possible synergetic antibacterial mechanism of MAl-LDHs was revealed: (1) MAl-LDHs altered the physicochemical properties of surroundings at high concentration of nanoparticles. (2) MAl-LDHs enhanced adhesion towards the membrane of bacteria. And (3) MAl-LDHs enhanced the local concentration of ROS and metal ions on the bacterial surface and morphology-dependent inhibition towards bacteria. Future studies will examine the contribution of MAl-LDHs on disruption of cell membrane, DNA/plasmid and proteins/enzymes *etc.* to reveal antibacterial mechanisms at cellular and molecular levels [48–51].

In conclusion, MAl-LDHs were prepared by a facile method. All of the MAl-LDHs had typical layered structures except for MnAl-LDH with M_3O_4 phases. MnAl-LDH with ellipsoids, spherical and rod-like structure and CuAl-LDH with rod-like shape existed particular morphology. Compared with the reported pure LDHs and clays, antibacterial activity of CuAl-LDH, NiAl-LDH, CoAl-LDH, and MnAl-LDH towards *E. coli* and *S. aureus* resulted in lower IC_{50} values of ~800-1500 μg/mL in broth tests. And antibacterial activity of CuAl-LDH, CoAl-LDH, and MnAl-LDH resulted in lower dosages of ~150–300 μg/disk with >10 mm inhibition zone in disk tests. The effective antimicrobial efficacy of MAl-LDHs could be attributed to the synergistic effects (effected surroundings, surface interactions, morphology of particles, ROS and metal ions). The simple approach proposed in this work could be extended to prepare inorganic LDHs based nanomaterials with high antimicrobial efficacy in water treatment and antibacterial coating industries.

Declaration of competing interest

The authors declare that they have no known competing financial interests or personal relationships that could have appeared to influence the work reported in this paper.

Acknowledgments

The authors thank associate facilities and the technical assistance of the Australian Microscopy & Microanalysis Research Facility at the Centre for Microscopy and Microanalysis (CMM) and Australian National Fabrication Facility (Qld Node), The University of Queensland. The study was financially supported by Advance Queensland Research Fellowship Project and Chinese Scholarship Council (CSC).

Appendix A. Supplementary data

Supplementary material related to this article can be found, in the online version, at doi:https://doi.org/10.1016/j.cclet.2019.09.047.

References

[1] P.C. Ray, S.A. Khan, A.K. Singh, D. Senapati, Z. Fan, Chem. Soc. Rev. 41 (2012) 3193–3209.
[2] N. Nishat, S. Ahmad, R.T. Ahamad, J. Appl. Polym. Sci. 100 (2006) 928–936.
[3] J. Xia, W. Wang, X. Hai, et al., Chin. Chem. Lett. 30 (2019) 421–424.
[4] X.R. Wang, H.M. Cheng, X.W. Gao, et al., Chin. Chem. Lett. 30 (2019) 919–923.
[5] M.R. Bindhu, M. Umadevi, Spectrochim. Acta A 135 (2015) 373–378.
[6] D.G. Evans, X. Duan, Chem. Commun. (2006) 485–496.
[7] B. Zumreoglu-Karan, A.N. Ay, Chem. Pap. 66 (2012) 1–10.
[8] F. Peng, D. Wang, D. Zhang, H. Cao, X. Liu, Appl. Clay Sci. 165 (2018) 179–187.
[9] M. Lobo-Sánchez, G. Nájera-Meléndez, G. Luna, et al., Appl. Clay Sci. 153 (2018) 61–69.
[10] Y. Qiao, Q. Li, H. Chi, et al., Appl. Clay Sci. 163 (2018) 119–128.
[11] Q.X. Li, H.A. Tang, Y.Z. Li, et al., J. Inorg. Biochem. 78 (2000) 167–174.
[12] D. Wang, N. Ge, S. Qian, et al., RSC Adv. 5 (2015) 106848–106859.
[13] M.G. Nair, M. Nirmala, K. Rekha, A. Anukaliani, Mater. Lett. 65 (2011) 1797–1800.
[14] R. Saravanan, M.M. Khan, V.K. Gupta, et al., RSC Adv. 5 (2015) 34645–34651.
[15] N.J. Hallab, C. Vermes, C. Messina, et al., J. Biomed. Mater. Res. 60 (2002) 420–433.
[16] Z.P. Xu, G. Stevenson, C.Q. Lu, G.Q. Lu, J. Phys. Chem. B 110 (2006) 16923–16929.
[17] L. Lv, P. Sun, Z. Gu, et al., J. Hazard. Mater. 161 (2009) 1444–1449.
[18] Z.P. Xu, J. Zhang, M.O. Adebajo, H. Zhang, C. Zhou, Appl. Clay Sci. 53 (2011) 139–150.

[19] R. Extremera, I. Pavlovic, M.R. Perez, C. Barriga, Chem. Eng. J. 213 (2012) 392–400.
[20] F. Kovanda, T. Rojka, P. Bezdicka, et al., J. Solid State Chem. 182 (2009) 27–36.
[21] L.H. Zhang, F. Li, D.G. Evans, X. Duan, Mater. Chem. Phys. 87 (2004) 402–410.
[22] S. Velu, K. Suzuki, T. Osaki, Catal. Lett. 69 (2000) 43–50.
[23] J.F. Lamonier, A.B. Boutoundou, C. Gennequin, et al., Catal. Lett. 118 (2007) 165–172.
[24] Y. Li, J. Qu, F. Gao, et al., Appl. Catal. B-Environ. 162 (2015) 268–274.
[25] Z.P. Xu, G.S. Stevenson, C.Q. Lu, et al., J. Am. Chem. Soc. 128 (2006) 36–37.
[26] R.H. Muller, C. Jacobs, O. Kayser, Adv. Drug Deliv. Rev. 47 (2001) 3–19.
[27] L.E. Dong, G.J. Gou, X.Q. Jin, M. Zhang, Chin. Chem. Lett. 25 (2014) 923–928.
[28] K.M. Reddy, K. Feris, J. Bell, et al., Appl. Phys. Lett. 90 (2007) 213902.
[29] Z.P. Xu, H.C. Zeng, J. Phys. Chem. B 105 (2001) 1743–1749.
[30] Z. Li, M. Shao, L. Zhou, et al., Nano Energy 20 (2016) 294–304.
[31] Y.H. Kim, D.K. Lee, H.G. Cha, et al., J. Phys. Chem. B 110 (2006) 24923–24928.
[32] S.K. Apte, S.D. Naik, R.S. Sonawane, et al., Mater. Res. Bull. 41 (2006) 647–654.
[33] G. Burygin, B. Khlebtsov, A. Shantrokha, et al., Nanoscale Res. Lett. 4 (2009) 794–801.
[34] S.C. Londono, H.E. Hartnett, L.B. Williams, Environ. Sci. Technol. 51 (2017) 2401–2408.
[35] D. Placha, K. Rosenbergova, J. Slabotinsky, et al., J. Hazard. Mater. 271 (2014) 65–72.
[36] S.E. Haydel, C.M. Remenih, L.B. Williams, J. Antimicrob. Chemother. 61 (2008) 353–361.
[37] L.A. Savas, M. Hancer, Appl. Clay Sci. 108 (2015) 40–44.
[38] S.M. Magana, P. Quintana, D.H. Aguilar, et al., J. Mol. Catal. A-Chem. 281 (2008) 192–199.
[39] C. Marambio-Jones, E.M.V. Hoek, J. Nanopart. Res. 12 (2010) 1531–1551.
[40] M.J. Hajipour, K.M. Fromm, A.A. Ashkarran, et al., Trends Biotechnol. 30 (2012) 499–511.
[41] R. Brayner, R. Ferrari-Iliou, N. Brivois, et al., Nano Lett. 6 (2006) 866–870.
[42] S.J. Ryu, H. Jung, J.M. Oh, J.K. Lee, J.H. Choy, J. Phys. Chem. Solids 71 (2010) 685–688.
[43] M.T. Qamar, M. Aslam, Z.A. Rehan, et al., Appl. Catal. B-Environ. 201 (2017) 105–118.
[44] H. Yang, C. Liu, D. Yang, H. Zhang, Z. Xi, J. Appl. Toxicol. 29 (2009) 69–78.
[45] G.B. Bagihalli, P.G. Avaji, S.A. Patil, P.S. Badami, Eur. J. Med. Chem. 43 (2008) 2639–2649.
[46] W.L. Du, S.S. Niu, Y.L. Xu, Z.R. Xu, C.L. Fan, Carbohydr. Polym. 75 (2009) 385–389.
[47] M. Li, Y. Sultanbawa, Z.P. Xu, et al., Colloids Surf. B: Biointerfaces 174 (2019) 435–442.
[48] N. Padmavathy, R. Vijayaraghavan, J. Biomed. Nanotechnol. 7 (2011) 813–822.
[49] F. Arabi, M. Imandar, M. Negahdary, et al., Ann. Biol. Res. 3 (2012) 3679–3685.
[50] N. Zhou, Z. Zhao, H. Wang, et al., Environ. Pollut. 252 (2019) 960–966.
[51] M. Zheng, N. Zhou, S. Liu, et al., J. Clean. Prod. 213 (2019) 365–374.